utilize E6AP to target p53 and other cellular proteins for degradation contributes to its oncogenic functions [Matentzoglu and Scheffner, 2008]. Interestingly, E6AP is not involved in the ubiquitylation of p53 in the absence of E6 [Talis et al., 1998].

In an attempt to understand the physiological function of E6AP, several potential E6-independent substrates for E6AP have been identified, such as HHR23A and HHR23B (the human orthologs of *Saccharomyces cerevisae* Rad23) [Kumar et al., 1999], Blk (a member of the Src family kinases) [Oda et al., 1999], Mcm7 (which is involved in DNA replication) [Kuhne and Banks, 1998], trihydrophobin 1 [Yang et al., 2007], and AIB1 (a steroid receptor coactivator) [Mani et al., 2006]. We previously reported that E6AP mediates ubiquitylation and degradation of annexin A1 in a Ca^{2+}-dependent manner [Shimoji et al., 2009].

Some patients with Angelman syndrome, a severe neurological disorder linked to E6AP, have mutations within the catalytic cleft that have been shown to reduce E6AP ubiquitin ligase activity [Kishino et al., 1997; Matsuura et al., 1997; Cooper et al., 2004]. Despite the significant progress in the study of Angelman syndrome-associated E6AP mutations, none of the identified E6AP substrates have been directly linked to the disorder. Much research is still needed to fully understand the functional links between lack of E6AP expression and clinical manifestations of Angelman syndrome [Dan, 2009]. We previously reported that E6AP mediates ubiquitin-dependent proteasomal degradation of hepatitis C virus (HCV) core protein, thereby affecting the production of HCV particles [Shirakura et al., 2007; Suzuki et al., 2009]. It is becoming increasingly clear that E6AP plays important roles in human diseases, such as cervical cancer, Angelman syndrome, and hepatitis C [Scheffner et al., 1993; Kishino et al., 1997; Shirakura et al., 2007].

In this study, we attempted to identify the novel functions of E6AP. We screened for potential binding partners for E6AP. A tandem affinity purification procedure coupled with mass spectrometry analysis identified peroxiredoxin 1 (Prx1) as a novel binding partner for E6AP. We provide evidence suggesting that E6AP mediates the ubiquitin-dependent proteasomal degradation of Prx1.

MATERIALS AND METHODS

CELL CULTURE AND TRANSFECTION

Human embryonic kidney (HEK) 293T cells were cultured in Dulbecco's modified Eagle's medium (DMEM; Sigma–Aldrich, St. Louis, MO) supplemented with 50 IU/ml penicillin, 50 μg/ml streptomycin (Invitrogen, Carlsbad, CA), and 10% (v/v) fetal bovine serum (FBS; JRH Biosciences, Lenexa, KS) at 37°C in a 5% CO_2 incubator. HEK293T cells were transfected with plasmid DNA using TransIT-LT1 (Mirus, Madison, WI).

PLASMIDS AND RECOMBINANT BACULOVIRUSES

To make a fusion protein consisting of hexahistidine (His_6)-tag fused to the N-terminus of Prx1 in *Escherichia coli*, pET17b-Prx1 [Kang et al., 1998] was digested with *Nde*I and *Bam*HI, and a Prx1 fragment was subcloned into the *Nde*I-Bpu1120I site of pET19b, resulting in pET19b-Prx1. The expression plasmid pET19b-Prx2 was constructed similarly. The plasmids, pET17b-Prx1 and pET17b-Prx2, were kind gifts from Dr. S.G. Rhee, Ewha Women's University, Korea.

To express the Prx1 protein as a FLAG-tagged fusion protein in mammalian cells, pCAG-FLAG-Prx1 was constructed as follows. The DNA fragment of Prx1 was amplified from pET17b-PrxI by polymerase chain reaction (PCR) using two oligonucleotides, 5′-GCGGCCGCCCACCATGGACTACAAAGACGATGACGATAAAGG-AGGCGGCGGATCCATGTCTTCAGGAAATGC-3′ and 5′-AGATCTT-CACTTCTGCTTGGAG-3′. To express FLAG-tagged Prx2 protein in mammalian cells, the DNA fragment of Prx2 was amplified from pET17b-Prx2 by PCR using two oligonucleotides, 5′-GCGGCCG-CCCACCATGGACTACAAAGACGATGACGATAAAGGAGGCGGCG-GATCCATGGCCTCCGGTAACGC-3′ and 5′-AGATCTCTAATTGTG-TTTGGAG-3′. The amplified PCR fragments were subcloned into pGEM T-Easy (Promega, Madison, WI) and verified by sequencing. Then the Prx1 and Prx2 gene fragments were digested with *Not*I and *Bgl*II, and ligated into the *Not*I–*Bgl*II site of pCAG-MCS2 [Shirakura et al., 2007]. The MEF-tag cassette (containing Myc-tag, the tobacco etch virus protease cleavage site, and FLAG-tag) was fused to the N-terminus of the cDNA encoding E6AP [Ichimura et al., 2005; Shirakura et al., 2007]. MEF-tagged E6AP and MEF-tagged E6AP C-A were subcloned into pcDNA3, pCAGGS, and pVL1392. pCAG-HA-E6AP, pCAG-HA-E6AP C-A, and pCAG-HA-Nedd4 were described previously [Shirakura et al., 2007; Shimoji et al., 2009]. The ubiquitin expression plasmids, pRK5-HA-Ubiquitin wild type (WT), pRK5-HA-Ubiquitin-K48R, and pRK5-HA-Ubiquitin-K48 [Lim et al., 2005], were provided by Dr. T. Dawson (Johns Hopkins University, MD).

ANTIBODIES

The mouse monoclonal antibodies (MAbs) used in this study were anti-hemagglutinin (HA) MAb (12CA5; Roche, Mannheim, Germany), anti-HA MAb (16B12; Covance, Princeton, NJ), anti-FLAG M2 mouse MAb (Sigma–Aldrich), anti-glyceraldehyde-3-phosphate dehydrogenase (GAPDH) MAb (Chemicon, Temecula, CA), anti-E6AP MAb (E6AP-330; Sigma–Aldrich), and anti-polyhistidine (His-1) MAb (Sigma–Aldrich). The c-Myc tagged protein mild purification kit (MBL) was used for immunoprecipitation. The polyclonal antibodies (PAbs) used in this study were anti-HA rabbit PAb (Y-11; Santa Cruz Biotechnology, Santa Cruz, CA), anti-FLAG rabbit PAb (F7425; Sigma–Aldrich), anti-Prx1 rabbit PAb (ab16805-100) (Abcam, Cambridge, Oxford), and anti-GST goat PAb (Amersham, Buckinghamshire, UK).

EXPRESSION AND PURIFICATION OF RECOMBINANT PROTEINS

E. coli BL21 (DE3) cells were transformed with plasmids expressing His_6-tagged protein and grown at 37°C. Expression of the fusion protein was induced by 1 mM isopropyl-β-D-thiogalactopyranoside (IPTG) at 25°C for 4 h. Bacteria were harvested, suspended in lysis buffer [50 mM Na_2HPO_4, 300 mM NaCl, 5 mM Imidazole, 0.1% Triton X-100, protease inhibitor cocktail (Complete EDTA-free; Roche)], and sonicated on ice. His_6-tagged proteins were purified on Ni-NTA beads (Qiagen, Hilden, Germany) according to the manufacturer's protocols. The MEF-E6AP and MEF-E6AP C-A were purified on anti-FLAG M2 agarose beads (Sigma–Aldrich) as described previously [Shirakura et al., 2007].

PURIFICATION OF E6AP-BINDING PROTEINS BY MEF PURIFICATION PROCEDURE

HEK293T cells were transfected with the plasmid expressing MEF-E6AP C-A by the calcium phosphate precipitation method, and the E6AP-binding proteins were recovered following the procedure described previously [Ichimura et al., 2005]. The inactive form of E6AP was expressed to inhibit ubiquitin-dependent degradation of potential substrates. Bound proteins were separated by 7.5% sodium dodecyl sulfate–polyacrylamide gel electrophoresis (SDS–PAGE) and visualized by silver staining. The stained bands were excised and digested in the gel with lysylendoprotease-C (Lys-C), and the resulting peptide mixtures were analyzed using a direct nanoflow liquid chromatography-tandem mass spectrometry (MS/MS) system, equipped with an electrospray interface reversed-phase column, a nanoflow gradient device, a high-resolution Q-time of flight hybrid mass spectrometer (Q-TOF2; Micromass, Manchester, UK), and an automated data analysis system [Natsume et al., 2002; Shirakura et al., 2007]. All the MS/MS spectra were searched against the nonredundant protein sequence database maintained at the National Center for Biotechnology Information using the Mascot program (Matrix Science, London, UK) to identify proteins. The MS/MS signal assignments were also confirmed manually.

Ni-NTA PULL-DOWN ASSAY

For Ni-NTA pull-down assays, purified MEF-E6AP was incubated with His_6-Prx proteins immobilized on Ni-NTA agarose beads (Qiagen) in 1 ml of the binding buffer [50 mM Tris–HCl (pH 7.5), 10% glycerol, 1% Triton X-100, 150 mM NaCl, 5 μM $ZnCl_2$, 1 mM Na_3VO_4, 10 mM EGTA, protease inhibitor cocktail (Complete EDTA-free)] at 4°C for 30 min. The beads were washed four times with wash buffer [50 mM Na_2HPO_4, 300 mM NaCl, 50 mM Imidazole, 0.1% Triton X-100, protease inhibitor cocktail (Complete EDTA-free)], and the pull-down complexes were separated by SDS–PAGE on 12.5% polyacrylamide gels and analyzed by immunoblotting with anti-FLAG MAb and anti-polyhistidine (His-1) MAb.

IMMUNOFLUORESCENCE MICROSCOPY

Cells were transfected with pCAG-HA-E6AP C-A and pCAG-FLAG-Prx1 using TransIT-LT1 according to the manufacturer's instructions. Transfected cells grown on collagen-coated coverslips were washed with PBS, fixed with 4% paraformaldehyde for 30 min at 4°C, and permeabilized with PBS containing 2% FCS and 0.3% Triton X-100. Cells were incubated with anti-HA mouse MAb and anti-FLAG rabbit PAb as primary antibodies, washed, and incubated with Alexa Fluor 488 goat anti-mouse IgG (Molecular Probes, Eugene, OR) and Alexa Fluor 555 goat anti-rabbit IgG (Molecular Probes) as secondary antibodies. Then, the cells were washed with PBS, mounted on glass slides, and examined with a BZ-8000 microscope (Keyence).

siRNA TRANSFECTION

HEK293T cells (3×10^5 cells in a six-well plate) were transfected with 40 pmol of either E6AP-specific small interfering RNA (siRNA; Sigma–Aldrich), or scramble negative-control siRNA duplexes (Sigma–Aldrich) using HiPerFect transfection reagent (Qiagen) following the manufacturer's instructions. The E6AP-siRNA target sequences were as follows:

siE6AP-1 (sense), 5′-GGGUCUACACCAGAUUGCUTT-3′; scramble negative control (siCont-1, sense), 5′-UUGCGGGUCUAAUCACCGATT-3′ [Shirakura et al., 2007].

IN VIVO UBIQUITYLATION ASSAY

In vivo ubiquitylation assays were performed essentially as described previously [Shirakura et al., 2007]. Where indicated, cells were treated with 25 μM MG132 (Calbiochem, La Jolla, CA) or with dimethylsulfoxide (DMSO; control) for 30 min prior to collection. FLAG-Prx1 was immunoprecipitated with anti-FLAG MAb. Immunoprecipitates were analyzed by immunoblotting, using either anti-HA PAb or anti-FLAG MAb to detect ubiquitylated Prx1.

IN VITRO UBIQUITYLATION ASSAY

In vitro ubiquitylation assays were performed essentially as described previously [Shirakura et al., 2007]. For in vitro ubiquitylation of Prx1, purified His_6-Prx1 was used as a substrate. Assays were done in 40-μl volumes containing 20 mM Tris–HCl, pH 7.6, 50 mM NaCl, 5 mM $MgCl_2$, 5 mM ATP, 8 μg of bovine ubiquitin (Sigma–Aldrich), 0.1 mM DTT, 200 ng of mouse E1, 200 ng of E2 (UbcH7), and 0.5 μg of MEF-E6AP. The reaction mixtures were incubated at 37°C for 120 min followed by immunoprecipitation with anti-Prx1 PAb. The samples were analyzed by immunoblotting with anti-Ub MAb.

RESULTS

IDENTIFICATION OF Prx1 AS A BINDING PARTNER FOR E6AP

To identify novel substrates for E6AP, we screened for E6AP-binding proteins using a tandem affinity purification procedure with a tandem tag (known as MEF-tag) [Ichimura et al., 2005; Shirakura et al., 2007]. Seven proteins were reproducibly detected from lysed cells transfected with MEF-E6AP C-A (Fig. 1A, lane 2), but none were recovered from lysed control cells transfected with empty vector alone (Fig. 1A, lane 1). To identify the proteins, silver-stained bands were excised from the gel, digested with Lys-C, and analyzed using a direct nanoflow liquid chromatography-MS/MS system. One of these bands, migrating at 25 kDa (Fig. 1A, lane 2, No. 7), was identified as Prx1 based on two independent MS spectra (Fig. 1B,C). To confirm the proteomic identification of Prx1, HEK293T cells were transfected with MEF-E6AP C-A plasmid or empty plasmid. The cells were lysed and immunoprecipitated with anti-Myc MAb or control IgG. Endogenous Prx1 was co-immunoprecipitated with anti-Myc MAb, suggesting that E6AP binds endogenous Prx1 (Fig. 1D, lane 4).

IN VIVO INTERACTION BETWEEN Prx1 AND E6AP

To determine whether E6AP specifically interacts with Prx1, HA-E6AP plasmid was introduced into HEK293T cells together with either FLAG-Prx1 plasmid or FLAG-Prx2 plasmid. Prx1 and Prx2 share 77.4% sequence identity at the protein level. Cells were lysed and immunoprecipitated with anti-HA MAb, anti-FLAG MAb, or

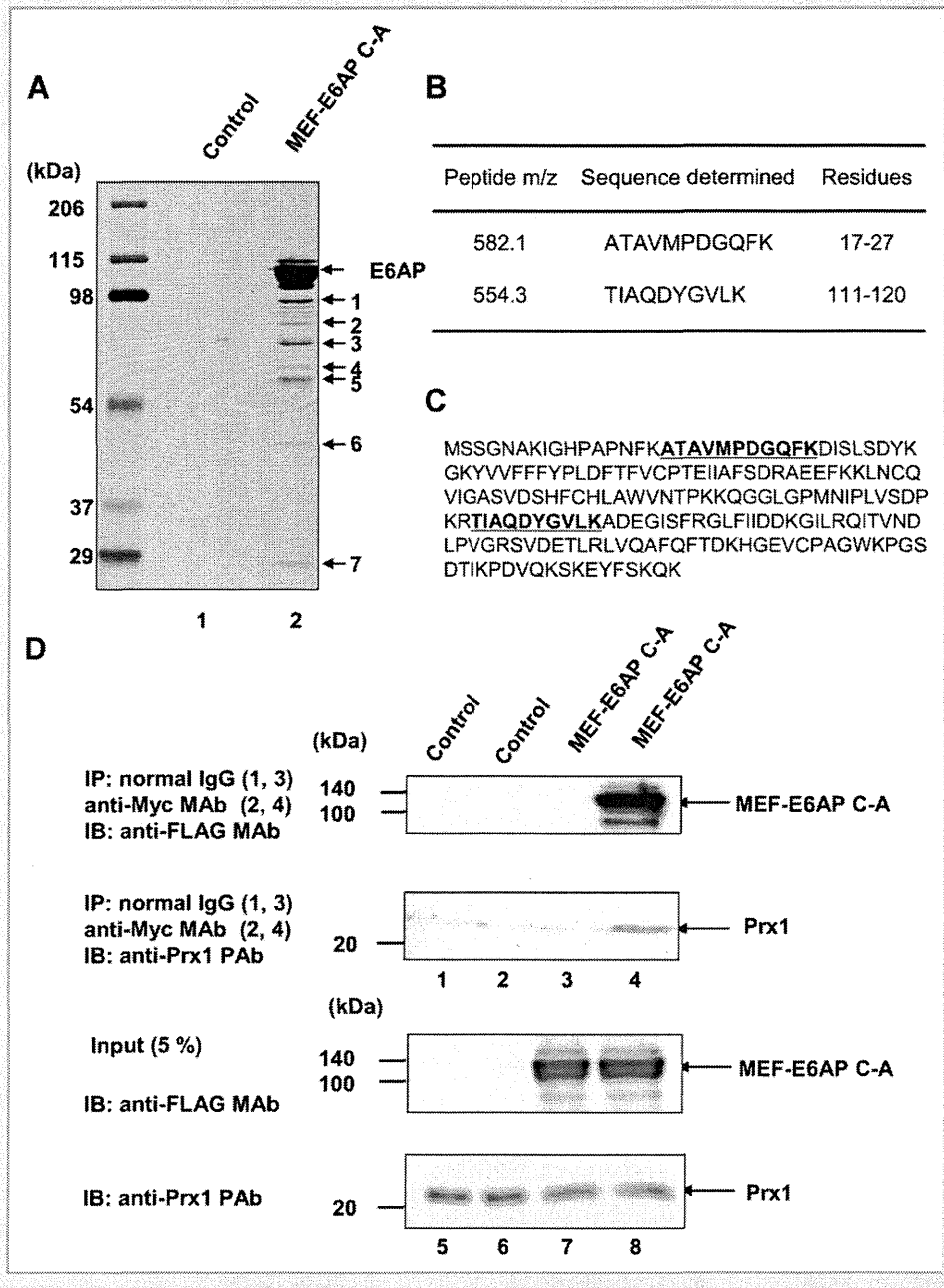

Fig. 1. Identification of Prx1 as a binding partner for E6AP. A: Prx1 interacts with E6AP in vivo. HEK293T cells were transfected with pcDNA3-MEF-E6AP C-A or empty plasmid, incubated for 48 h, and then harvested. The expressed MEF-E6AP C-A and binding proteins were recovered using the MEF purification procedure. Proteins bound to the MEF-E6AP C-A immobilized on anti-FLAG beads were dissociated with FLAG peptides, resolved by 7.5% SDS–PAGE, and visualized by silver staining. Control experiments were performed using HEK293T cells transfected with vector alone. Bound proteins were detected by SDS–PAGE and silver staining. Molecular weight markers are indicated as well as the position of p25 (No. 7), which likely corresponds to Prx1. B: Peptide masses were identified by tandem mass spectrometry. The protein was Prx1 (GenBank accession No. BC021683). C: Corresponding amino acids of Prx1 (peptides in bold print). D: HEK293T cells were co-transfected with MEF-E6AP C-A plasmid. Control experiments were performed using HEK293T cells transfected with vector alone. Cell lysates were immunoprecipitated with anti-Myc MAb or normal mouse IgG (lanes 1–4), eluted with c-Myc tag peptide. Eluates were analyzed by immunoblotting with anti-FLAG MAb or anti-Prx1 PAb. The input samples were separated by SDS–PAGE and analyzed by immunoblotting with anti-FLAG MAb or anti-Prx1 PAb (lanes 5–8). The positions of Prx1 and MEF-E6AP C-A are indicated by arrows. IB, immunoblot; IP, immunoprecipitation.

normal IgG (Fig. 2A, lanes 1–6). FLAG-Prx1 but not FLAG-Prx2 was co-immunoprecipitated with anti-HA MAb (Fig. 2A, lower panel, lanes 1 and 2). Conversely, HA-E6AP was co-immunoprecipitated with FLAG-Prx1 but not FLAG-Prx2 using anti-FLAG MAb (Fig. 2A, upper panel, lanes 3 and 4). These results suggest that E6AP specifically interacts with Prx1.

To determine whether Prx1 and E6AP co-localize in the cells, immunofluorescence microscopy analysis was performed in HEK293T cells. There was no staining without primary antibodies (data not shown). The immunofluorescence study showed that E6AP and Prx1 mainly localize in the cytoplasm and that E6AP and Prx1 co-localize in the cytoplasm (Fig. 2B, Merge).

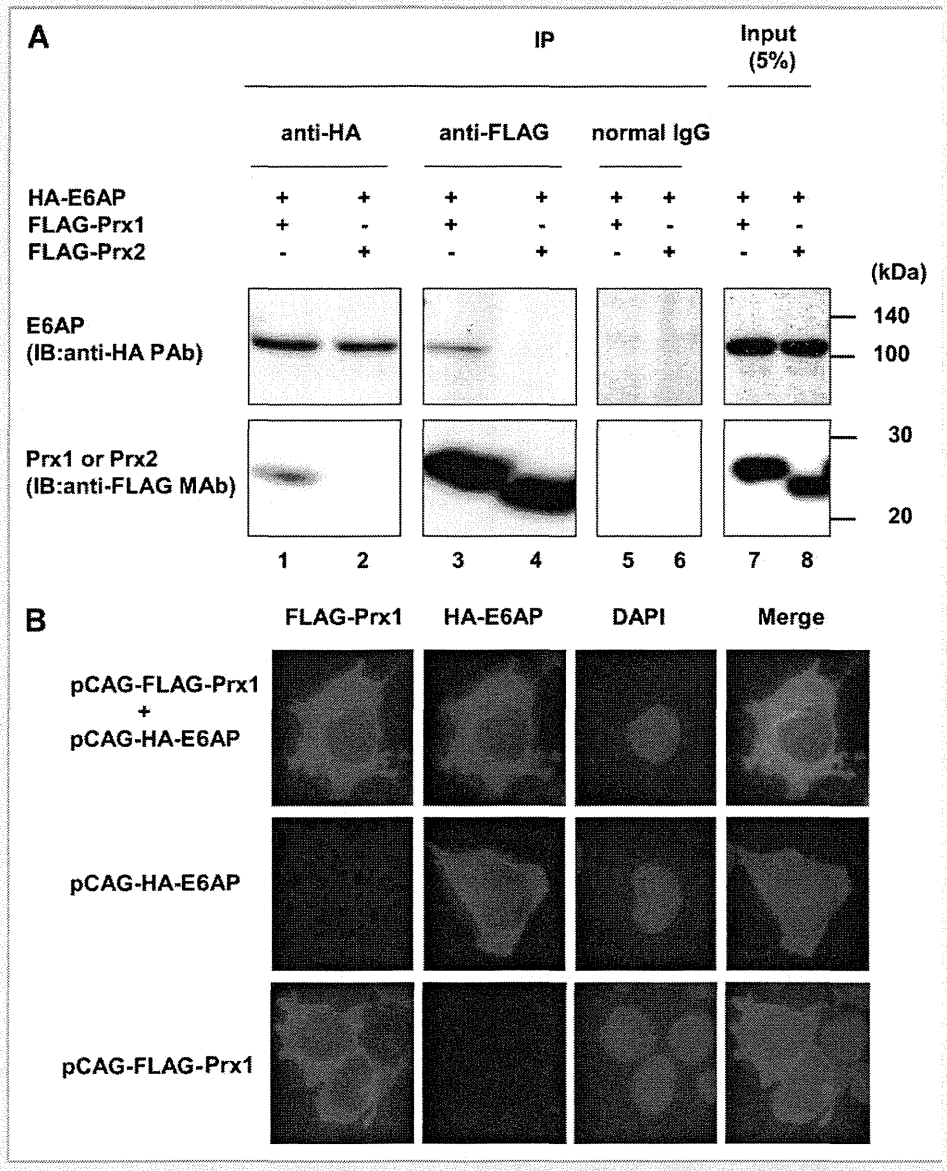

Fig. 2. In vivo interaction between Prx1 and E6AP. A: HEK293T cells were co-transfected with pCAG-HA-E6AP together with either pCAG-FLAG-Prx1 or pCAG-FLAG-Prx2. Cell lysates were immunoprecipitated with anti-HA mouse MAb, anti-FLAG mouse MAb, or normal mouse IgG and analyzed by immunoblotting with anti-HA PAb or anti-FLAG MAb. B: HEK293T cells were transfected with either HA-E6AP plasmid or FLAG-Prx1 plasmid, grown on coverslips, fixed, and processed for double-label immunofluorescence for HA-E6AP or FLAG-Prx1. All the samples were examined with a BZ-8000 microscope (Keyence).

IN VITRO INTERACTION BETWEEN Prx1 AND E6AP

To determine whether E6AP interacts with Prx1 in vitro, purified recombinant MEF-E6AP, MEF-annexin A1 expressed in insect cells using a baculovirus system and purified recombinant His_6-Prx1 and His_6-Prx2 expressed in *E. coli* were used. The His_6-tagged Prx proteins were mixed with either MEF-E6AP or MEF-annexin A1, incubated, pulled down with Ni-NTA agarose, and analyzed by immunoblotting with anti-FLAG MAb (Fig. 3, upper panel) or anti-polyhistidine MAb (Fig. 3, middle panel). MEF-annexin A1 served as a negative control to confirm that MEF-tag does not bind Prx1. MEF-E6AP was pulled down with Prx1, but not with Prx2 (Fig. 3, lanes 1 and 3), whereas annexin A1 was not pulled down with either Prx1 or Prx2 (Fig. 3, lanes 2 and 4). These results suggest that E6AP directly and specifically binds Prx1 in vitro.

E6AP DECREASES STEADY-STATE LEVELS OF Prx1 IN HEK293T CELLS

One of the characteristic features of HECT domain ubiquitin ligases is their direct association with their substrates. Thus, we hypothesized that E6AP would function as an E3 ubiquitin ligase for Prx1. We assessed the effects of E6AP on the steady-state levels of Prx1 in HEK293T cells. FLAG-Prx1 together with HA-tagged E6AP, catalytically inactive E6AP, E6AP C-A, or Nedd4 (another HECT domain ubiquitin ligase) was introduced into HEK293T cells, and the levels of Prx1 were examined by immunoblotting. The steady-state

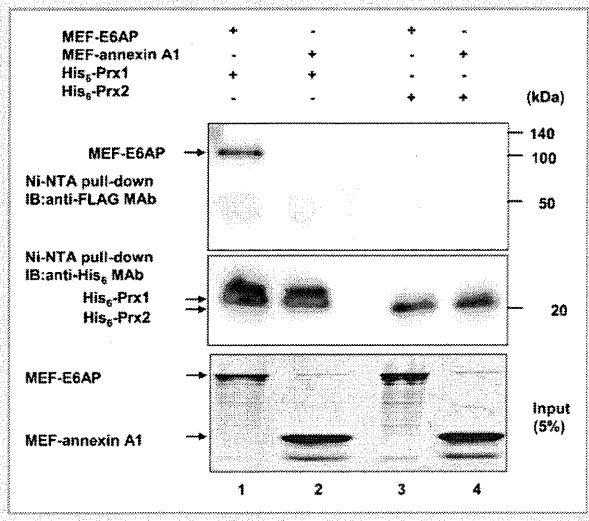

Fig. 3. In vitro interaction between Prx1 and E6AP. Purified MEF-E6AP, MEF-Annexin A1, His_6-Prx1, and His_6-Prx2 were used to examine the interaction between E6AP and Prxs. Purified MEF-E6AP was mixed with either His_6-Prx1 or His_6-Prx2, incubated, and pulled down with Ni-NTA agarose. MEF-Annexin A1 served as a negative control. The bound proteins were separated by SDS-PAGE and analyzed by immunoblotting with anti-FLAG MAb (upper panel) or anti-His_6 MAb (middle panel). The input MEF-E6AP and MEF-annexin A1 were separated by SDS-PAGE and stained with Coomassie brilliant blue (lower panel).

levels of Prx1 decreased with an increase in the amount of E6AP plasmid (Fig. 4A lanes 1–3, Fig. 4B). However, neither E6AP C-A nor Nedd4 decreased the steady-state levels of Prx1 (Fig. 4A lanes 4–6 and 7–9, Fig. 4B), indicating that E6AP specifically decreases Prx1.

To determine if endogenous E6AP is critical for the degradation of endogenous Prx1 in the cells, the expression of E6AP was knocked down by siRNA and the expression of Prx1 and E6AP was analyzed by immunoblotting. Transfection of siE6AP into HEK293T cells resulted in a decrease in E6AP levels by 97% (Fig. 4C, upper panel, lane 2). Knock-down of endogenous E6AP resulted in accumulation of endogenous Prx1 (Fig. 4C, lane 2, middle panel), suggesting that endogenous E6AP plays a role in the proteolysis of endogenous Prx1.

To further investigate if the E6AP-induced reduction of Prx1 is dependent on the proteasome, we examined the effects of the proteasome inhibitor clasto-lactacystin and the lysosomal enzyme inhibitors, E-64d and Pepstatin A, on the level of Prx1. Clasto-lactacystin was used to examine if Prx1 gets stabilized after the treatment, because it has an irreversible inhibitory effect on proteasome. HEK293T cells were transfected with pCAG-FLAG-Prx1 plus either empty vector or pCAG-HA-E6AP. Overexpression of E6AP resulted in a remarkable reduction of the Prx1 (Fig. 4D, lane 2, middle panel), whereas the Prx1 protein level was increased after treatment with clasto-lactacystin (Fig. 4D, lane 4, middle panel). In contrast, the Prx1 protein level was unchanged after treatment with E-64d plus Pepstatin A (Fig. 4D, lane 6, middle panel). These results indicate that E6AP-induced reduction of Prx1 is proteasome-dependent.

E6AP-DEPENDENT POLYUBIQUITYLATION OF Prx1 IN VIVO

To determine whether E6AP can induce ubiquitylation of Prx1 in cells, we performed in vivo ubiquitylation assays. HEK293T cells were transfected with FLAG-Prx1 plasmid and either E6AP or Nedd4 plasmid, together with a plasmid encoding HA-tagged ubiquitin to facilitate the detection of ubiquitylated Prx1. Cell lysates were immunoprecipitated with anti-FLAG MAb and immunoblotted with anti-HA PAb to detect ubiquitylated Prx1 protein. No ubiquitin signal was detected in the cells co-transfected with empty plasmid or Nedd4 plasmid (Fig. 5A, lanes 4 and 6). In contrast, co-expression of E6AP led to readily detectable polyubiquitylated forms of the Prx1 as a smear of higher-molecular weight bands (Fig. 5A, left panel, lane 5). Immunoblot analysis with anti-FLAG PAb confirmed that FLAG-Prx1 was immunoprecipitated and that higher-molecular weight bands conjugated with HA-ubiquitin were indeed poly-ubiquitylated forms of the FLAG-Prx1 (Fig. 5A, right panel, lane 5). These results suggest that E6AP enhances polyubiquitylation of Prx1 in vivo.

To further investigate if E6AP is involved in K48-linked ubiquitylation of Prx1, we performed in vivo ubiquitylation assay using HA-tagged K48R dominant negative ubiquitin mutant and K48 only ubiquitin mutant expression plasmids. HEK293T cells were transfected with FLAG-Prx1 plasmid and E6AP plasmid, together with a plasmid encoding HA-ubiquitin WT, HA-K48R ubiquitin, or HA-K48 ubiquitin to facilitate the detection of ubiquitylated Prx1. Ubiquitin signal was detected in the cells transfected with either HA-ubiquitin WT or HA-K48 ubiquitin plasmid (Fig. 5B, lane 1 or 3), whereas no ubiquitin signal was detected in the cells transfected with HA-K48R ubiquitin (Fig. 5B, lane 2), suggesting that E6AP enhances K48-linked polyubiquitylation of Prx1. These results are consistent with the notion that E6AP is involved in proteasomal degradation of Prx1.

E6AP MEDIATES POLYUBIQUITYLATION OF Prx1 IN VITRO

To reconstitute the E6AP-mediated polyubiquitylation of Prx1 in vitro, we performed an in vitro ubiquitylation assay of the Prx1 using purified MEF-E6AP and His_6-Prx1 as described above. When the in vitro ubiquitylation reaction was carried out in the presence of MEF-E6AP C-A, no ubiquitylation signal was detected (Fig. 5C, lanes 3). However, inclusion of purified MEF-E6AP in the reaction mixture resulted in ubiquitylation of His_6-Prx1 (Fig. 5C, lane 4). No signal was detected when His_6-Prx1 was not included in the reaction mixture (Fig. 5C, lane 2). From these results, we concluded that E6AP mediates polyubiquitylation of Prx1.

DISCUSSION

In this study, we identified Prx1 as a novel E6AP-binding protein using a tandem affinity purification procedure coupled with mass spectrometry. Overexpression of E6AP enhances proteasomal degradation of Prx1, and siRNA-mediated knockdown of endogenous E6AP results in accumulation of endogenous Prx1. E6AP enhances the polyubiquitylation of Prx1 in vivo and in vitro. We conclude that E6AP mediates ubiquitin-dependent degradation of

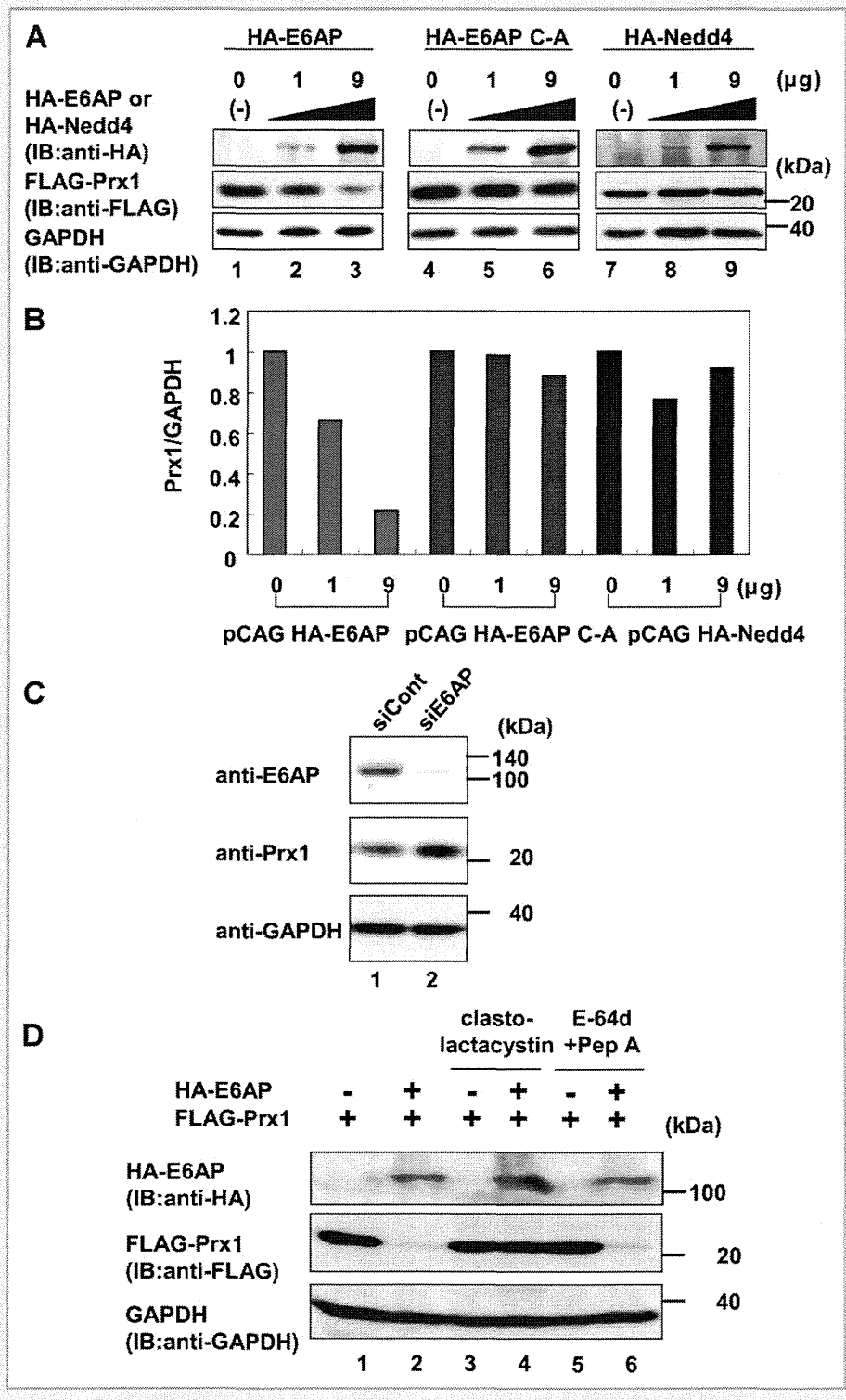

Fig. 4. E6AP decreases the steady-state levels of Prx1 protein in HEK293T cells. A: HEK293T cells (5×10^5 cells/six-well plate) were transfected with 0.5 μg pCAG-FLAG-Prx1 plus empty vector and 1 or 9 μg of pCAG-HA-E6AP, pCAG-HA-E6AP C-A, or pCAG-HA-Nedd4. At 48 h posttransfection, equivalent amounts of the whole-cell lysates were separated by SDS-PAGE and analyzed by immunoblotting with anti-HA MAb (top panel), anti-FLAG MAb (middle panel), and anti-GAPDH MAb (bottom panel). The results shown are representative of three independent experiments. B: Quantitation of the data shown in panel A. The intensities of the gel bands were quantitated using the ImageJ 1.43 program. The level of GAPDH served as a loading control. C: Knockdown of endogenous E6AP by siRNA resulted in the accumulation of endogenous Prx1 in HEK293T cells. HEK293T cells (3×10^5 cells/six-well plate) were transfected with 40 pmol of E6AP-specific duplex siRNA (or a scramble negative control). The cells were harvested at 96 h after siRNA transfection. D: HEK293T cells (5×10^5 cells/six-well plate) were transfected with 0.5 μg of pCAG-FLAG-Prx1 plus 9 μg of empty vector or pCAG-HA-E6AP. At 36 h after transfection, the cells were treated with DMSO control (lanes 1 and 2), 30 μM clasto-lactacystin (lanes 3 and 4), or 40 μM E-64d plus 20 μM Pepstatin A (lanes 5 and 6). Cells were collected at 12 h after treatment with the inhibitors. Equivalent amounts of the whole-cell lysates were separated by SDS-PAGE and analyzed by immunoblotting with anti-HA MAb (upper panel), anti-FLAG MAb (middle panel), or anti-GAPDH MAb (lower panel).

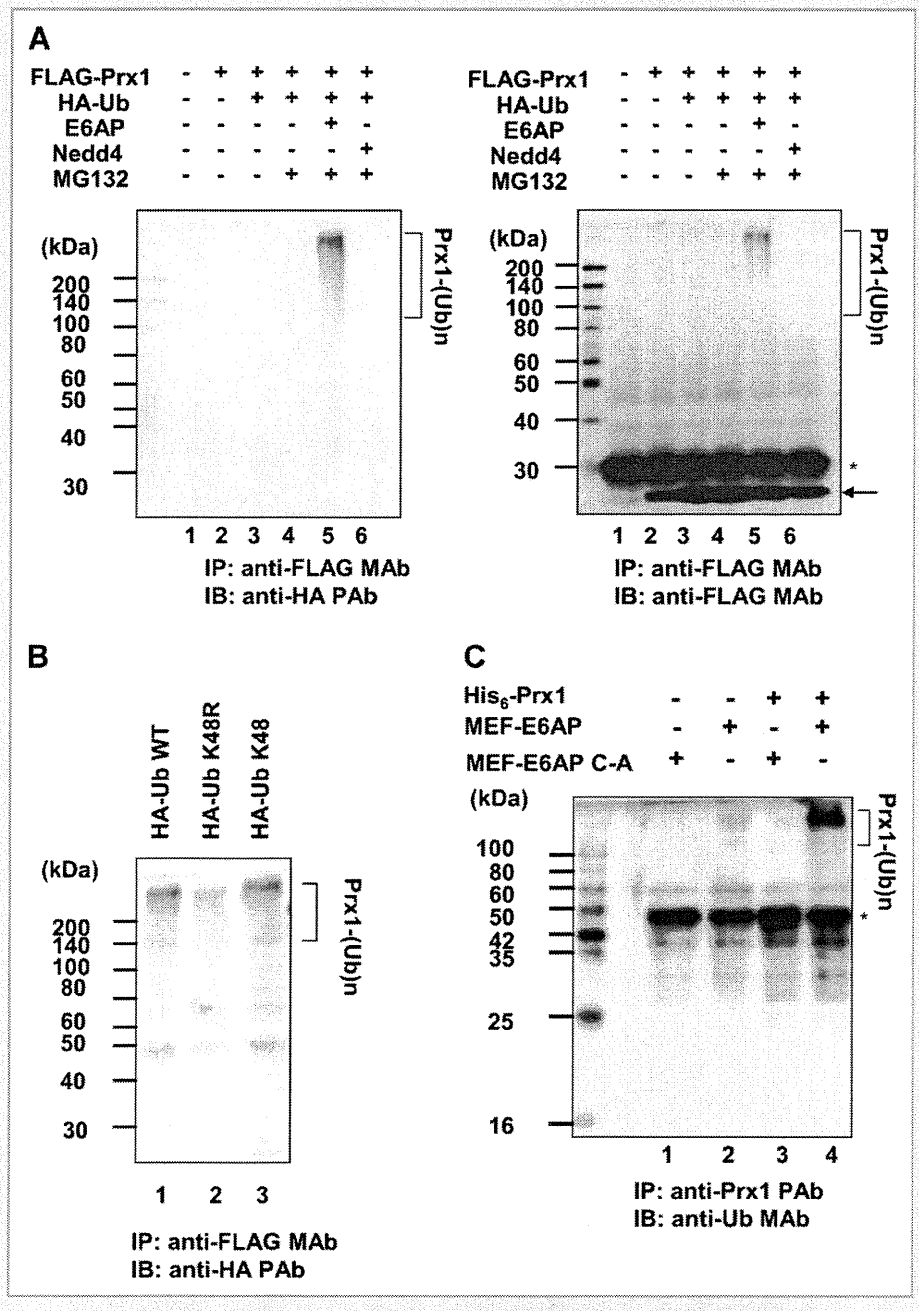

Fig. 5. E6AP mediates ubiquitylation of Prx1 in vivo and in vitro. A: HEK293T cells (2×10^6 cells/10-cm dish) were transfected with 1 μg of pCAG-FLAG-Prx1 together with 2 μg of plasmid encoding E6AP or Nedd4 as indicated. Each transfection also included 2 μg of plasmid encoding HA-ubiquitin. The cell lysates were immunoprecipitated with FLAG beads and analyzed by immunoblotting with anti-HA PAb (left panel) or anti-FLAG MAb (right panel). Arrow indicates FLAG-Prx1. Asterisk indicates immunoglobulin light chain. Ubiquitylated species of FLAG-Prx1 are marked by brackets. B: HEK293T cells (2×10^6 cells/10-cm dish) were transfected with 1 μg of pCAG-FLAG-Prx1 together with 2 μg of plasmid encoding E6AP plasmid. Each transfection also included 2 μg of plasmid encoding HA-Ub WT, HA-Ub K48R, or HA-Ub K48 as indicated. At 36 h after transfection, the cells were treated with 25 μM MG132 and cultured for 12 h. The cell lysates were immunoprecipitated with FLAG beads and analyzed by immunoblotting with anti-HA PAb. Ubiquitylated species of FLAG-Prx1 are marked by brackets. C: In vitro ubiquitylation of Prx1 by recombinant E6AP. For in vitro ubiquitylation of Prx1 protein, purified His_6-Prx1 was used as a substrate. Assays were done in 40-μl volumes containing each component as indicated. The reaction mixture is described in Materials and Methods Section. The reaction was carried out at 37°C for 120 min followed by immunoprecipitation with anti-Prx1 PAb and analysis by immunoblotting with anti-Ub MAb. Ubiquitylated species of His_6-Prx1 are marked by brackets. Asterisk indicates immunoglobulin heavy chain.

Prx1. Our results suggest that E6AP is involved in the regulation of Prx1 activity through the ubiquitin–proteasome pathway.

Prx1 is a 25-kDa member of the Prx family, a ubiquitous family of antioxidant peroxidases that regulate many cellular processes through intracellular oxidative signal transduction pathways. More than 50 members of the Prx family have been identified in a wide variety of organisms ranging from prokaryotes to mammals. Prxs are widely expressed hydrogen peroxide scavenger proteins best

known for their role in detoxifying reactive oxygen species, DNA damage, and cancer, but they also act in cellular signaling and as molecular chaperones [Jang et al., 2004; Hall et al., 2009]. Mammalian cells express six isoforms of Prx (Prx1-6), which are classified into three subgroups (2-Cys, atypical 2-Cys, and 1-Cys) [Rhee et al., 2005]. Prx1 is a 2-Cys thiol reductase that forms a component of cellular antioxidant and thermal stress defense mechanisms through its ability to metabolize H_2O_2, and its properties as a molecular chaperone [Wood et al., 2003a,b; Jang et al., 2004]. Furthermore, Prx1 controls neuronal differentiation by a thiol-redox-dependent cascade [Yan et al., 2009].

The peroxidase activity of Prx1 is regulated by phosphorylation, which is mediated by cyclin-dependent kinases [Chang et al., 2002]. Phosphorylation at Thr90 by several Cdks, including Cdc2, results in inhibition of its peroxidase activity. Another known regulatory mechanism is cysteine sulfinic acid formation [Woo et al., 2003]. The active-site cysteine of Prx1 is selectively reduced to cysteine sulfinic acid during catalysis, which leads to inactivation of peroxidase activity. Reversing the inactivation of Prx1 was previously identified as a mechanism for its regulation. The sulfinic form of Prx1, produced during the exposure of cells to H_2O_2, is rapidly reduced to the catalytic active thiol form [Woo et al., 2003]. We propose here a novel regulatory mechanism of Prx1. Our results show for the first time that the E6AP-mediated ubiquitin-proteasome pathway is a mechanism for irreversibly attenuating the activity of Prx1. Our data suggest that E6AP specifically targets Prx1 for ubiquitin-dependent proteasomal degradation. Prx1 and Prx2 share 77.4% sequence identity at the protein level. However, our data showed that E6AP does not interact with Prx2 in vivo and in vitro, suggesting a specific interaction between E6AP and Prx1.

Angelman syndrome is a neurologic disorder characterized by developmental delay, severe intellectual disability, motor impairment, absent speech, happy demeanor, and epilepsy, and is attributed to an absence of UBE3A/E6AP gene expression that may be caused by various abnormalities of chromosome 15. Although the genetic link between UBE3A/E6AP and Angelman syndrome was identified more than 13 years ago [Kishino et al., 1997; Matsuura et al., 1997], the underlying pathophysiology is poorly understood. Ubiquitin-mediated proteolysis may be important in a number of processes of neuronal development, including synaptogenesis and mechanisms of long-term memory. Recent findings in animal models of Angelman syndrome have demonstrated altered dendritic spine formation as well as both synaptic and nonsynaptic influences in various brain regions, including hippocampus and cerebellar cortex [Dan, 2009]. Yan et al. [2009] provided several lines of evidence suggesting that the requirement for Prx1 in motor neuron differentiation stems from a previously uncharacterized enzymatic function that is distinct from its molecular chaperone or H_2O_2 metabolic activities. It may be intriguing to investigate the functional link between lack of UBE3A/E6AP expression and stability of Prx1 with regard to the pathogenesis of Angelman syndrome.

The expression of Prx1 is induced by oxidative stress including that from the exposure to O^2, Fe^{3+}, or 2-mercaptoethanol. In addition to H_2O_2, other chemicals such as phorbol ester and okadaic acid have also been shown to induce the expression of Prx1 [Immenschuh et al., 2002; Wijayanti et al., 2008]. Increased expression of Prx1, in turn, contributes to greater resistance to oxidative stress. Many studies have indicated that aberrant expression of Prx1 was found in various kinds of cancers, such as thyroid tumors, oral cancers, lung cancers, and esophageal carcinoma [Yanagawa et al., 1999; Yanagawa et al., 2000; Chang et al., 2001; Qi et al., 2005]. As the hypoxic and unstable oxygenation microenvironment of a tumor is one of the key factors influencing tumor growth and progression, the induction of Prx1 expression might be an adaptive response of the cancer cells [Zhang et al., 2009]. Although the molecular mechanism responsible for the abnormal elevation of Prx1 is still unclear, it may be interesting to investigate the gene polymorphisms of E6AP and the stability of Prx1 in cancer cells.

There are several modes of substrate recognition in the ubiquitin-proteasome system. Recognition can be made via several mechanisms, such as (1) NH_2-terminal residues (the N-end rule pathway), (2) allosteric activation, (3) recognition of phosphorylated substrate, (4) phosphorylation of E3, (5) phosphorylation of both the ligase and its substrate, (6) recognition in trans via an ancillary protein, (7) abnormal/mutated/misfolded proteins, and (8) recognition via hydroxylated protein [Glickman and Ciechanover, 2002]. It is known that E6AP uses several mechanisms for substrate recognition. E6AP recognizes p53 in conjunction with the HPV16 E6 protein [Scheffner et al., 1993; Talis et al., 1998]. E6AP also recognizes the tyrosine-phosphorylated form of Blk [Oda et al., 1999] and the Ca^{2+}-binding form of annexin A1 [Shimoji et al., 2009]. Further studies will be needed to elucidate the mode of Prx1 recognition by E6AP.

In conclusion, we demonstrated that E6AP mediates the ubiquitin-dependent degradation of Prx1. Future efforts will focus on understanding the role of the E6AP-mediated proteolysis of Prx1 in the defense against oxidative stress and thermal stress as well as the ubiquitylation signal of Prx1. Insights into the physiological function of E6AP will be gained by investigating the effects of various oxidative stresses on the stability and functional control of Prx1.

ACKNOWLEDGMENTS

We thank Dr. Bohmann (EMBL) for providing pMT123 and Dr. Iwai (Osaka University) for recombinant baculovirus carrying His_6-mouse E1. We also thank T. Mizoguchi and K. Hachida for secretarial work. This work was supported in part by a grant from the 100th Anniversary of the Foundation of the Nippon Dental University; by a grant for Research on Health Sciences focusing on Drug Innovation from the Japan Health Sciences Foundation; by grants-in-aid from the Ministry of Health, Labour, and Welfare; by a grant from the Ministry of Education, Science and Culture of Japan; by the program for Promotion of Fundamental Studies in Health Sciences of the National Institute of Biomedical Innovation (NIBIO), Japan.

REFERENCES

Chang JW, Jeon HB, Lee JH, Yoo JS, Chun JS, Kim JH, Yoo YJ. 2001. Augmented expression of peroxiredoxin I in lung cancer. Biochem Biophys Res Commun 289:507-512.

Chang TS, Jeong W, Choi SY, Yu S, Kang SW, Rhee SG. 2002. Regulation of peroxiredoxin I activity by Cdc2-mediated phosphorylation. J Biol Chem 277:25370–25376.

Cooper EM, Hudson AW, Amos J, Wagstaff J, Howley PM. 2004. Biochemical analysis of Angelman syndrome-associated mutations in the E3 ubiquitin ligase E6-associated protein. J Biol Chem 279:41208–41217.

Dan B. 2009. Angelman syndrome: Current understanding and research prospects. Epilepsia 50:2331–2339.

Gewin L, Myers H, Kiyono T, Galloway DA. 2004. Identification of a novel telomerase repressor that interacts with the human papillomavirus type-16 E6/E6-AP complex. Genes Dev 18:2269–2282.

Glickman MH, Ciechanover A. 2002. The ubiquitin-proteasome proteolytic pathway: Destruction for the sake of construction. Physiol Rev 82:373–428.

Hall A, Karplus PA, Poole LB. 2009. Typical 2-Cys peroxiredoxins—Structures, mechanisms and functions. FEBS J 276:2469–2477.

Huibregtse JM, Scheffner M, Howley PM. 1993. Cloning and expression of the cDNA for E6-AP, a protein that mediates the interaction of the human papillomavirus E6 oncoprotein with p53. Mol Cell Biol 13:775–784.

Huibregtse JM, Scheffner M, Beaudenon S, Howley PM. 1995. A family of proteins structurally and functionally related to the E6-AP ubiquitin-protein ligase. Proc Natl Acad Sci USA 92:2563–2567.

Ichimura T, Yamamura H, Sasamoto K, Tominaga Y, Taoka M, Kakiuchi K, Shinkawa T, Takahashi N, Shimada S, Isobe T. 2005. 14-3-3 proteins modulate the expression of epithelial Na+ channels by phosphorylation-dependent interaction with Nedd 4-2 ubiquitin ligase. J Biol Chem 280: 13187–13194.

Immenschuh S, Iwahara S, Schwennen B. 2002. Induction of heme-binding protein 23/peroxiredoxin I gene expression by okadaic acid in cultured rat hepatocytes. DNA Cell Biol 21:347–354.

Jang HH, Lee KO, Chi YH, Jung BG, Park SK, Park JH, Lee JR, Lee SS, Moon JC, Yun JW, Choi YO, Kim WY, Kang JS, Cheong GW, Yun DJ, Rhee SG, Cho MJ, Lee SY. 2004. Two enzymes in one; Two yeast peroxiredoxins display oxidative stress-dependent switching from a peroxidase to a molecular chaperone function. Cell 117:625–635.

Kang SW, Baines IC, Rhee SG. 1998. Characterization of a mammalian peroxiredoxin that contains one conserved cysteine. J Biol Chem 273: 6303–6311.

Kishino T, Lalande M, Wagstaff J. 1997. UBE3A/E6-AP mutations cause Angelman syndrome. Nat Genet 15:70–73.

Kuhne C, Banks L. 1998. E3-ubiquitin ligase/E6-AP links multicopy maintenance protein 7 to the ubiquitination pathway by a novel motif, the L2G box. J Biol Chem 273:34302–34309.

Kumar S, Talis AL, Howley PM. 1999. Identification of HHR23A as a substrate for E6-associated protein-mediated ubiquitination. J Biol Chem 274:18785–18792.

Lim KL, Chew KC, Tan JM, Wang C, Chung KK, Zhang Y, Tanaka Y, Smith W, Engelender S, Ross CA, Dawson VL, Dawson TM. 2005. Parkin mediates nonclassical, proteasomal-independent ubiquitination of synphilin-1: Implications for Lewy body formation. J Neurosci 25:2002–2009.

Mani A, Oh AS, Bowden ET, Lahusen T, Lorick KL, Weissman AM, Schlegel R, Wellstein A, Riegel AT. 2006. E6AP mediates regulated proteasomal degradation of the nuclear receptor coactivator amplified in breast cancer 1 in immortalized cells. Cancer Res 66:8680–8686.

Matentzoglu K, Scheffner M. 2008. Ubiquitin ligase E6-AP and its role in human disease. Biochem Soc Trans 36:797–801.

Matsuura T, Sutcliffe JS, Fang P, Galjaard RJ, Jiang YH, Benton CS, Rommens JM, Beaudet AL. 1997. De novo truncating mutations in E6-AP ubiquitin-protein ligase gene (UBE3A) in Angelman syndrome. Nat Genet 15:74–77.

Nakagawa S, Huibregtse JM. 2000. Human scribble (Vartul) is targeted for ubiquitin-mediated degradation by the high-risk papillomavirus E6 proteins and the E6AP ubiquitin-protein ligase. Mol Cell Biol 20:8244–8253.

Natsume T, Yamauchi Y, Nakayama H, Shinkawa T, Yanagida M, Takahashi N, Isobe T. 2002. A direct nanoflow liquid chromatography-tandem mass spectrometry system for interaction proteomics. Anal Chem 74:4725–4733.

Oda H, Kumar S, Howley PM. 1999. Regulation of the Src family tyrosine kinase Blk through E6AP-mediated ubiquitination. Proc Natl Acad Sci USA 96:9557–9562.

Qi Y, Chiu JF, Wang L, Kwong DL, He QY. 2005. Comparative proteomic analysis of esophageal squamous cell carcinoma. Proteomics 5:2960–2971.

Rhee SG, Chae HZ, Kim K. 2005. Peroxiredoxins: A historical overview and speculative preview of novel mechanisms and emerging concepts in cell signaling. Free Radic Biol Med 38:1543–1552.

Scheffner M, Huibregtse JM, Vierstra RD, Howley PM. 1993. The HPV-16 E6 and E6-AP complex functions as a ubiquitin-protein ligase in the ubiquitination of p53. Cell 75:495–505.

Scheffner M, Huibregtse JM, Howley PM. 1994. Identification of a human ubiquitin-conjugating enzyme that mediates the E6-AP-dependent ubiquitination of p53. Proc Natl Acad Sci USA 91:8797–8801.

Shimoji T, Murakami K, Sugiyama Y, Matsuda M, Inubushi S, Nasu J, Shirakura M, Suzuki T, Wakita T, Kishino T, Hotta H, Miyamura T, Shoji I. 2009. Identification of annexin A1 as a novel substrate for E6AP-mediated ubiquitylation. J Cell Biochem 106:1123–1135.

Shirakura M, Murakami K, Ichimura T, Suzuki R, Shimoji T, Fukuda K, Abe K, Sato S, Fukasawa M, Yamakawa Y, Nishijima M, Moriishi K, Matsuura Y, Wakita T, Suzuki T, Howley PM, Miyamura T, Shoji I. 2007. E6AP ubiquitin ligase mediates ubiquitylation and degradation of hepatitis C virus core protein. J Virol 81:1174–1185.

Suzuki R, Moriishi K, Fukuda K, Shirakura M, Ishii K, Shoji I, Wakita T, Miyamura T, Matsuura Y, Suzuki T. 2009. Proteasomal turnover of hepatitis C virus core protein is regulated by two distinct mechanisms: A ubiquitin-dependent mechanism and a ubiquitin-independent but PA28gamma-dependent mechanism. J Virol 83:2389–2392.

Talis AL, Huibregtse JM, Howley PM. 1998. The role of E6AP in the regulation of p53 protein levels in human papillomavirus (HPV)-positive and HPV-negative cells. J Biol Chem 273:6439–6445.

Wijayanti N, Naidu S, Kietzmann T, Immenschuh S. 2008. Inhibition of phorbol ester-dependent peroxiredoxin I gene activation by lipopolysaccharide via phosphorylation of RelA/p65 at serine 276 in monocytes. Free Radic Biol Med 44:699–710.

Woo HA, Chae HZ, Hwang SC, Yang KS, Kang SW, Kim K, Rhee SG. 2003. Reversing the inactivation of peroxiredoxins caused by cysteine sulfinic acid formation. Science 300:653–656.

Wood ZA, Poole LB, Karplus PA. 2003a. Peroxiredoxin evolution and the regulation of hydrogen peroxide signaling. Science 300:650–653.

Wood ZA, Schroder E, Robin Harris J, Poole LB. 2003b. Structure, mechanism and regulation of peroxiredoxins. Trends Biochem Sci 28:32–40.

Yan Y, Sabharwal P, Rao M, Sockanathan S. 2009. The antioxidant enzyme Prdx1 controls neuronal differentiation by thiol-redox-dependent activation of GDE2. Cell 138:1209–1221.

Yanagawa T, Ishikawa T, Ishii T, Tabuchi K, Iwasa S, Bannai S, Omura K, Suzuki H, Yoshida H. 1999. Peroxiredoxin I expression in human thyroid tumors. Cancer Lett 145:127–132.

Yanagawa T, Iwasa S, Ishii T, Tabuchi K, Yusa H, Onizawa K, Omura K, Harada H, Suzuki H, Yoshida H. 2000. Peroxiredoxin I expression in oral cancer: A potential new tumor marker. Cancer Lett 156:27–35.

Yang Y, Liu W, Zou W, Wang H, Zong H, Jiang J, Wang Y, Gu J. 2007. Ubiquitin-dependent proteolysis of trihydrophobin 1 (TH1) by the human papilloma virus E6-associated protein (E6-AP). J Cell Biochem 101:167–180.

Zhang B, Wang Y, Su Y. 2009. Peroxiredoxins, a novel target in cancer radiotherapy. Cancer Lett 286:154–160.

Journal of Medical Virology 82:1364–1370 (2010)

Secondary Structure of the Amino-Terminal Region of HCV NS3 and Virological Response to Pegylated Interferon Plus Ribavirin Therapy for Chronic Hepatitis C

Mai Sanjo,[1] Takafumi Saito,[1]* Rika Ishii,[1] Yuko Nishise,[1] Hiroaki Haga,[1] Kazuo Okumoto,[1] Junitsu Ito,[1] Hisayoshi Watanabe,[1] Koji Saito,[1] Hitoshi Togashi,[2] Kazuto Fukuda,[3] Yasuharu Imai,[3] Ahmed El-Shamy,[4] Lin Deng,[4] Ikuo Shoji,[4] Hak Hotta,[4] and Sumio Kawata[1]

[1]*Department of Gastroenterology, Yamagata University School of Medicine, Yamagata, Japan*
[2]*Health Administrative Center, Yamagata University, Yamagata, Japan*
[3]*Division of Gastroenterology, Ikeda Municipal Hospital, Osaka, Japan*
[4]*Division of Microbiology, Kobe University Graduate School of Medicine, Kobe, Japan*

The aim of the study was to identify a predictive marker for the virological response in hepatitis C virus 1b (HCV-1b)-infected patients treated with pegylated interferon plus ribavirin therapy. A total of 139 patients with chronic hepatitis C who received therapy for 48 weeks were enrolled. The secondary structure of the 120 residues of the amino-terminal HCV-1b non-structural region 3 (NS3) deduced from the amino acid sequence was classified into two major groups: A and B. The association between HCV NS3 protein polymorphism and virological response was analyzed in patients infected with group A ($n = 28$) and B ($n = 40$) isolates who had good adherence to both pegylated interferon and ribavirin administration (>95% of the scheduled dosage) for 48 weeks. A sustained virological response (SVR) representing successful HCV eradication occurred in 33 (49%) in the 68 patients. Of the 28 patients infected with the group A isolate, 18 (64%) were SVR, whereas of the 40 patients infected with the group B isolate only 15 (38%) were SVR. The proportion of virological responses differed significantly between the two groups ($P < 0.05$). These results suggest that polymorphism in the secondary structure of the HCV-1b NS3 amino-terminal region influences the virological response to pegylated interferon plus ribavirin therapy, and that virus grouping based on this polymorphism can contribute to prediction of the outcome of this therapy. ***J. Med. Virol. 82:1364–1370, 2010.*** © 2010 Wiley-Liss, Inc.

KEY WORDS: hepatitis C; interferon; ribavirin; interaction; polymorphism

INTRODUCTION

Hepatitis C virus (HCV) is the major pathogen that causes chronic liver diseases with a risk of progression to cirrhosis and hepatocellular carcinoma. Currently, the standard treatment for chronic hepatitis C is antiviral therapy using pegylated interferon (Peg-IFN) plus ribavirin (RBV), and this approach is most effective for eradication of HCV viremia. However, even with the widely used treatment regimen of 48 weeks, the rate of sustained virological response (SVR), which indicates eradication of viremia, is still approximately 50% for patients infected with the therapy-resistant HCV genotype 1b (HCV-1b) with a high viral load [Manns et al., 2001; Bruno et al., 2004; Hadziyannis et al., 2004]. It would be useful to predict the virological response to this therapy and to identify patients who would obtain beneficial therapeutic effects before treatment, in order to avoid any serious side effect and to eliminate those who would not be helped by the treatment. In the future it will be important to establish a protocol of tailor-made medicine for chronic hepatitis C.

Grant sponsor: Grant-in-Aid for Scientific Research; Grant number: 21590824; Grant sponsor: Global Center of Excellence program of the Japan Society for the Promotion of Science (Yamagata University School of Medicine and Kobe University Graduate School of Medicine); Grant sponsor: Ministry of Health, Labor and Welfare of Japan.

*Correspondence to: Takafumi Saito, M. D., Department of Gastroenterology, Yamagata University School of Medicine, 2-2-2 Iida-nishi, Yamagata 990-9585, Japan.
E-mail: tasaitoh@med.id.yamagata-u.ac.jp

Accepted 6 March 2010
DOI 10.1002/jmv.21818
Published online in Wiley InterScience (www.interscience.wiley.com)

Both the HCV genotype and pre-treatment viral load are major viral factors that influence the response to IFN-based antiviral therapy, but IFN resistance is also partly due to variation of the amino acid sequence encoded by HCV itself. Enomoto et al. [1996] proposed that variation of 40 amino acids within the NS5A region (aa 2,209–2,248), which is referred to as the IFN sensitivity-determining region (ISDR), is well correlated with IFN responsiveness. ISDR and its adjacent sequence bind and inhibit the enzymatic activity of a double-stranded RNA-activated protein kinase (PKR), which can have an antiviral effect, and therefore the combined region is referred to as the PKR-binding domain (PKR-BD) [Gale et al., 1997, 1998]. A correlation between sequence variation in the PKR-BD and IFN responsiveness has been reported [Nousbaum et al., 2000], and some reports show a correlation between IFN responsiveness and the sequence diversity of variable region 3 (V3) (aa 2,356–2,379) or surrounding regions near the carboxy terminus of NS5A [Murphy et al., 2002; Sarrazin et al., 2002; Puig-Basagoiti et al., 2005]. A high degree of amino acid substitution in the V3 and pre-V3 regions (aa 2,334–2,355) of NS5A, which is referred to as the IFN/RBV resistance-determining region (IRRDR) (aa 2,334–2,379), has been associated with SVR in Peg-IFN/RBV combination therapy for patients infected with HCV-1b [El-Shamy et al., 2007, 2008]. In addition to these findings in non-structural proteins of the virus, amino acid substitution in a structural region of HCV has been reported to be a predictive viral marker for the virological response to PegIFN/RBV therapy. Amino acid polymorphisms in the HCV core region (Arg70 vs. Gln70 and Leu91 vs. Met91) correlate with virological outcome and on-treatment viral kinetics in Peg-IFN/RBV therapy [Akuta et al., 2006, 2007], and a double wild-type HCV core (Arg70 and Leu91) may be a significant predictor of SVR in Peg-IFN/RBV therapy [Akuta et al., 2007].

Interactions between viral and host proteins in infected cells may influence therapeutic effects and the natural history of infection, since the HCV NS3 region has a significant effect on immunity. The amino-terminal part of this region encodes a serine protease, for which the minimum activity has been mapped to a region between aa 1,059 and 1,204 [Yamada et al., 1998]. The serine protease inactivates Cardif, a caspase recruitment domain (CARD)-containing adaptor protein that interacts with the RNA helicase retinoic acid inducible gene 1 (RIG-1)-dependent antiviral pathway in infected cells [Foy et al., 2003; Meylan et al., 2005; Evans and Seeger, 2006]. This action inhibits phosphorylation and subsequent heterodimerization of interferon regulatory factor-3 (IRF-3), which is essential for activation of IFN signaling through translocation of IRF-3 heterodimers into the nucleus, and eventually blocks IFN-beta production. In addition, inactivation of IRF-3 is postulated to influence the therapeutic effect of IFN-based antiviral therapy, because the IRF-3 heterodimer translocates into the nucleus to bind to the IFN-stimulated response element that produces many antiviral proteins, including 2′,5′-oligoadenylate synthetase and PKR [Nakaya et al., 2001; Grandvaux et al., 2002]. Collectively, these findings suggest that polymorphisms in HCV NS3 structure deduced from sequence variation may influence IFN-related signaling and the antiviral effect of IFN-based anti-HCV therapy.

We have focused on polymorphisms in the secondary structure of the viral polyprotein that interacts with host proteins involved in immunity, with the aim of identification of predictive viral markers for the response to Peg-IFN/RBV therapy. In this study, we examined the potential correlation between polymorphisms in the secondary structure of the HCV NS3 amino-terminal region and virological responses to Peg-IFN/RBV therapy in patients infected with HCV-1b with a high viral load.

PATIENTS AND METHODS

Patients and Treatment Regimen With Peg-IFN Plus Ribavirin

A total of 139 consecutive patients diagnosed with chronic hepatitis C were enrolled in the study from December 2004 to March 2007. These patients included 81 men and 58 women, and were aged from 31 to 75 years old (mean ± SD, 56.8 ± 8.7 years old). All patients were infected with HCV-1b with a high viral load of over 100 KIU/ml, and all received Peg-IFN/RBV therapy. Patients with alcoholic liver injury, autoimmune liver disease, and those who had symptoms of decompensated cirrhosis including ascites were excluded. Briefly, all patients were treated with a combination of Peg-IFN-alpha 2b (Pegintron®; Schering-Plough, Kenilworth, NJ) and RBV (Rebetol®; Schering-Plough) for 48 weeks. Peg-IFN was administered subcutaneously once a week and RBV was given orally twice a day for the total dose. The dosages were determined on the basis of body weight according to the Japanese standard prescription information supplied by the Japanese Ministry of Health, Labour and Welfare, and there was a limit for calculating the optimized dose: patients with body weights of 35–45, 46–60, 61–75, and 76–90 kg were given Peg-IFN at doses of 60, 80, 100, and 120 μg, respectively, and those with body weights of <60, 60–80, and >80 kg were given RBV at doses of 600, 800, and 1,000 mg, respectively. The dose of Peg-IFN or RBV was reduced according to the Japanese standard criteria based on the white blood cell count, neutrophil count, hemoglobin concentration and platelet count [Hiramatsu et al., 2008].

Virological Tests and Response to Peg-IFN Plus Ribavirin

Virological responses were evaluated at 12 weeks after the start of treatment with an early depletion of viremia referred to as an early virological response (EVR), at the end of treatment with depletion of viremia referred to as an end of treatment virological response (ETR), and at 24 weeks after completion of treatment,

with a clinical outcome of a sustained virological response (SVR) representing successful HCV eradication. All patients were negative for hepatitis B surface antigen. Quantification of serum HCV RNA was performed using an RT-PCR-based commercial kit (Amplicor HCV monitor test, ver. 2.0, Roche Diagnostics, Tokyo, Japan). This Amplicor HCV RNA assay has a lower limit of detection of 50 IU/ml. SVR was determined by monitering negativity for HCV RNA monthly for 6 months. The real-time PCR assay kit (COBAS TaqMan HCV Auto, Roche Diagnostics) for more precise quantitation of HCV viremia has recently become available and pre-treatment viral titers were re-evaluated using preserved serum samples. This real-time PCR assay has a lower limit of detection of 15 IU/ml. The study protocol was approved by the Ethics Committee of Yamagata University Hospital. Informed consent was obtained from all patients.

PCR Amplification of the Amino-Terminal Region of NS3

RNA was extracted from 50 μl of serum using an RNeasy Mini kit (Qiagen, Tokyo, Japan). To amplify the region of the HCV genome encoding the amino-terminal region of NS3 (1,027–1,206), a one-step PCR was performed in a tube using the Superscript One-Step RT-PCR kit with Platinum Taq (Gibco-BRL, Tokyo, Japan) and an outer set of primers: NS3-F1 (sense primer; 5′-ACA CCG CGG CGT GTG GGG ACA T-3′; nucleotides 3,295–3,316) and NS3-AS2 (antisense primer; 5′-GCT CTT GCC GCT GCC AGT GGG A-3′; nucleotides 4,040–4,019), as reported previously [Ogata et al., 2002a, 2003]. PCR was initially performed at 45°C for 30 min at RT and then at 94°C for 2 min, followed by the first-round PCR for forty 3-min cycles at 94°, 55°, and 72°C for 1 min each. The second-round PCR was performed with *Pfu* DNA polymerase (Promega, Tokyo, Japan) and an inner set of primers: NS3-F3 (sense primer; 5′-CAG GGG TGG CGG CTC CTT-3′; nucleotides 3,390–3,407) and NS3-AS1 (antisense primer; 5′-GCC ACT TGG AAT GTT TGC GGT A-3′; nucleotides 4,006–3,985). The second-round PCR was performed for 35 cycles, with each cycle consisting of 1 min at 94°C, 1.5 min at 55°C, and 3 min at 72°C. This method allowed amplification of the corresponding portion of the HCV genome from HCV-1b RNA-positive samples. The amplified fragments were purified with a QIAquick PCR purification kit (Qiagen) and directly sequenced (without being subcloned) in both directions using a dRhodamine Terminator Cycle Sequencing Ready Reaction kit and an ABI 377 sequencer (Applied Biosystems, Tokyo, Japan).

Classification of the Secondary Structure of the HCV-1b NS3 Amino-Terminal Region

The secondary structure of the amino-terminal region of HCV NS3 was predicted by computer-assisted Robson analysis [Garnier et al., 1978] with Genetyx-Mac software (ver.10.1; Software Development Co., Tokyo, Japan). Previously, the full-length secondary structure of the HCV-1b NS3 region was analyzed, and this showed that the secondary structure deduced from the carboxy-terminal 60 residues was well conserved in terms of linear structure, without any turn structure [Ogata et al., 2002a]. We have shown that the secondary structure of the 120 residues in the amino-terminal region of HCV-1b NS3 can be classified into two major groups: A and B (Fig. 1) [Ogata et al., 2002a, 2003]. Briefly, the criteria for this classification are as follows: in group A isolates, the carboxy-terminal 20 residues (aa 1,125–1,146) are oriented leftward relative to a domain composed of the remaining amino-terminal region; whereas in group B isolates, the same 20 residues are oriented rightward relative to the rest of the amino-terminal domain.

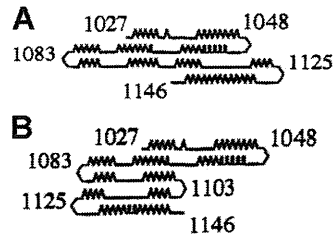

Fig. 1. Secondary structure of the 120 amino-terminal residues of HCV-1b nonstructural 3 (NS3) region classified into two major groups: A and B. The looped, zigzag, straight, and bent lines represent α-helix, β-sheet, coil, and turn structures, respectively. The numbers indicate amino acid positions. **A**: Group A, (**B**) Group B.

Analysis of Amino Acid Substitutions in the Core Region

To amplify a region of the HCV genome encoding the core region including positions 70 and 91, reverse transcription and the first-round PCR were performed in a tube by the Superscript One-Step RT-PCR kit with Platinum *Taq* (Gibco-BRL) and an outer set of primers, followed by second-round PCR with an inner set of primers in accordance with procedures reported previously [Ogata et al., 2002b]. The sequences of the amplified fragments were determined by direct sequencing.

Statistical Analysis

Data were analyzed by a χ^2 test for independence with a two-by-two contingency table and a Student t-test. A P-value <0.05 was considered significant.

RESULTS

Virological Response *and Adherence* to the Peg-IFN Plus Ribavirin Regimen

Rates of virological responses in patients treated with PegIFN/RBV combination therapy for 48 weeks are shown in Figure 2. Of the 139 patients enrolled in the study, SVR, non-SVR and cessation of therapy occurred in 58 (42%), 62 (45%), and 19 (14%), respectively. Serious

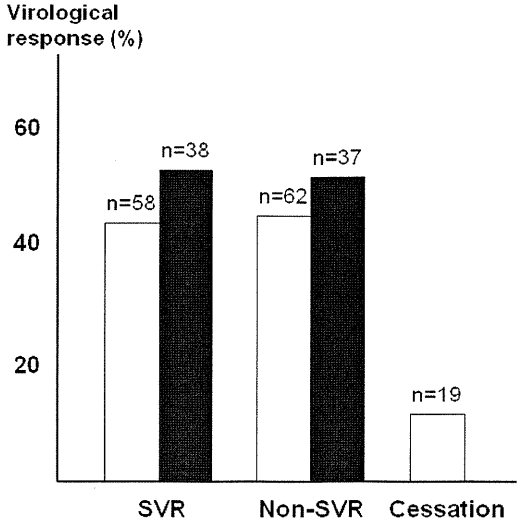

Fig. 2. Virological response in patients treated with peginterferon plus ribavirin for 48 weeks. The results are shown for all 139 subjects (open bars) and for 75 cases with good adherence of >80% of the scheduled dosages (closed bars). SVR, sustained virological response.

adverse events that necessitated discontinuation of this therapy were depression in one patient, thyroid function disorder in 2, general itching in 2, infection in 2, anorexia in 2, occurrence of hepatocellular carcinoma in 2, and a decreased neutrophil count in 2. Six patients also terminated this therapy at their own request. Of the 139 patients, 75 (54%) received >80% of the scheduled dosage of Peg-IFN and RBV designated before treatment, and of these 75 cases SVR and non-SVR occurred in 38 (51%) and 37 (49%), respectively.

Prevalence of Types of Secondary Structure of the Amino-Terminal Region of HCV NS3

The prevalence of the types of secondary structure of HCV NS3 in the 139 subjects is shown in Table I. Among these subjects, 43 (31%), 70 (50%), and 26 (19%) were classified into groups A, B, and others, including 3 of mixed type (A plus B) and 23 of non-A, non-B type. Of the 75 cases with good adherence to administration of >80% of the scheduled dosage, 28 (37%), 40 (53%) and 7 (9%) were classified into groups A, B, and others. The amino acid data of group A and B in the cases with good adherence to administration are available in the DDBJ/EMBL/GenBank databases with the accession numbers AB548070–AB548137. Our analysis revealed no specific correlations between amino acid sequences and the secondary structure deduced by the Robson method, as we have reported previously [Ogata et al., 2003].

TABLE I. Prevalence of the HCV NS3 Secondary Structure Type

	Group A (%)	Group B (%)	Others (%)
Enrolled cases (n = 139)	43 (31)	70 (50)	26 (19)
Adherent cases (n = 75)	28 (37)	40 (53)	7 (9)

Characteristics of Adherent Patients Based on Different HCV NS3 Structure Types

The virological responses to Peg-IFN/RBV combination therapy for patients infected with group A and B isolates were assessed in the 68 subjects with good adherence to the scheduled dosage of Peg-IFN and RBV. The characteristics of patients infected with group A and B isolates are shown in Table II. Age, gender, pre-treatment level of serum HCV RNA and ALT, and frequency of fibrosis stage did not differ significantly between the two groups. Peg-IFN/RBV combination therapy was completed in all the patients, and the total administered dosages of Peg-IFN and RBV was >95% of the scheduled dosage in both groups.

Relationship Between Virological Responses and Polymorphisms in the HCV NS3 Amino-Terminal Region

In the 68 patients who received >95% of the scheduled doses of Peg-IFN and RBV for 48 weeks, SVR and non-SVR occurred in 33 (49%) and 35 (51%), respectively. The EVR, ETR, and SVR rates in patients infected with group A and B isolates are shown in Table III. There was a significant difference in the rates of EVR between subjects infected with group A and B isolates: EVR was achieved in 19 of 28 (68%) patients with group A infection, compared to 17 of 40 (43%) with group B infection ($P < 0.05$). The final outcome also differed significantly between subjects infected with group A and B isolates: SVR was achieved in 18 of 28 (64%) patients with group A infection, compared to 15 of 40 (38%) with group B infection ($P < 0.05$).

Polymorphisms in Core Amino Acids 70/91 and in the HCV NS3 Secondary Structure

The wild-type core sequence (Arg70, Leu91) has been associated with SVR in Peg-IFN/RBV combination therapy, while the non-double wild-type containing one or two substitutions at positions 70 and/or 91 was associated with non-SVR [Akuta et al., 2007]. Therefore, we examined substitutions at positions 70 and 91 in the HCV core region in pre-treatment serum samples of 44 cases that were available for testing. The double wild-type 70/91 sequence was found in 22 of the 44 cases (50%), of which 12 were SVR and 10 were non-SVR. Combination analysis of polymorphisms of the HCV core 70/91 positions and the NS3 amino-terminal region showed that 10 (83%) of the 12 SVR cases and only 3 (30%) of the 10 non-SVR cases with the double wild-type core had a group A polymorphism in HCV NS3 (Table IV). Thus, combination analysis of the core and NS3 regions may improve prediction of the outcome of Peg-IFN/RBV therapy.

TABLE II. Characteristics of Adherent Patients Infected With HCV Group A and B Isolates

	Group A (n = 28)	Group B (n = 40)	P
Age (years)	55.5 ± 9.5	55.5 ± 8.9	NS[a]
Sex (men/women)	18/10	21/19	NS[b]
Pre-treatment HCV RNA (KIU/ml)	1,635 ± 930	2,087 ± 1,422	NS[a]
Alanine aminotransferase level (U/L)	80 ± 62	71 ± 47	NS[a]
Stage of liver fibrosis			
F1 or F2/F3 or F4	19/9	28/12	NS[b]
Drug adherence dosage (%)			
Pegylated interferon	97.7 ± 5.2	95.2 ± 7.3	NS[a]
Ribavirin	96.8 ± 6.4	95.3 ± 7.7	NS[a]

NS, not significant.
[a]*t*-test.
[b]χ^2 test.

Re-Evaluation of Pre-Treatment HCV Viremia Status Using Real-Time PCR

Since the viral titer before treatment is a major predictive marker of the outcome of Peg-IFN/RBV therapy, we re-evaluated the pre-treatment viral titers more precisely using preserved serum samples taken within 1 month before treatment, using a real-time PCR assay. The pre-treatment viral titers did not differ significantly between sera with group A and B isolates (5.98 ± 0.94 vs. 6.25 ± 0.62 logIU/ml) (Table V). The secondary structure polymorphisms of HCV NS3 were independent of the pre-treatment viral titers.

DISCUSSION

Antiviral therapy with Peg-IFN/RBV for 48 weeks fails to eradicate HCV in about half of patients infected with a high titer of HCV genotype 1b, and the severe adverse events and high costs associated with this therapy require outcome prediction to allow targeted treatment for chronic hepatitis C. The pre-treatment viral titer, viral factors that influence the virological response to IFN-based anti-HCV therapy have been widely investigated. Viral kinetics showing prompt seronegativity after the start of treatment is a critical factor for achieving SVR, and thus the possible correlation between an early virological response and genetic sequence variation of the HCV has been studied. In particular, amino acid substitutions in the HCV core region at positions 70 and 91 or multiple mutations detected in the IRRDR of the HCV NS5A region are useful markers for predicting EVR and subsequent SVR.

TABLE III. Virological Responses in Subjects With Different Polymorphisms in the Secondary Structure of HCV NS3

	EVR*	ETR**	SVR*
Group A (n = 28)	19 (68%)	23 (82%)	18 (64%)
Group B (n = 40)	17 (43%)	25 (63%)	15 (38%)

EVR: early virological response at 12 weeks after the start of treatment.
ETR: virological response at the end of treatment.
SVR: sustained virological response 24 weeks after completion of treatment.
*$P < 0.05$.
**$P = 0.08$; χ^2 test.

To date, the influence of several single amino acid substitutions and accumulation of these changes in the viral genome on the effect of IFN-based anti-HCV therapy has been examined. Since interactions between host and viral proteins in infected cells may influence the therapeutic effect of an antiviral agent, we focused on the association of structural polymorphism of a viral protein with the effect of Peg-IFN/RBV combination therapy in this study. Our results suggest that polymorphism analysis of secondary structure deduced from sequence variations in the HCV NS3 amino-terminal region can be used to predict viral responses to this therapy.

Amino acid sequences of the HCV NS3 amino-terminal region, which encodes a serine protease, vary greatly among HCV isolates. Interactions between HCV NS3 and host proteins may influence both oncogenesis and immunity, and thus elucidation of the biological significance of these interactions could result in a new prognostic marker for HCC or a predictive marker for anti-HCV therapy. First, HCV NS3 interacts with the p53 tumor suppressor to suppress p53-dependent apoptosis or p21 transcriptional activity [Ishido and Hotta, 1998; Kwun et al., 2001; Deng et al., 2006]. Transfection of a plasmid expressing the amino-terminal portion of HCV NS3 induces cell transformation in vitro, and transplanted cells proliferate with sarcoma-like features in vivo [Sakamuro et al., 1995]. These findings suggest that NS3 may be involved in the oncogenic pathway in HCV infection. We have shown that the secondary structure of the 120-residue amino-terminal region of NS3 (1,027–1,146) is classifiable into two major groups: A and B. This region encodes a serine protease and also includes p53-binding sites. Our

TABLE IV. Treatment Outcome of Cases With a Double Wild-Type Core Region and Different HCV NS3 Structural Polymorphism

	Group A (%)	Group B (%)	P
SVR (n = 12)	10 (83)	2 (17)	0.02[a]
Non-SVR (n = 10)	3 (30)	7 (70)	

SVR, sustained virological response.
[a]χ^2 test.

TABLE V. Pre-Treatment HCV RNA Levels Measured by Real-Time PCR for Subjects With Different HCV NS3 Structural Polymorphism

	Group A	Group B	*P*
SVR (n = 33)	5.78 ± 1.05	6.I3 ± 0.71	NS[a]
Non-SVR (n = 35)	6.33 ± 0.59	6.32 ± 0.55	NS[a]
Total (n = 68)	5.98 ± 0.94	6.25 ± 0.62	NS[a]

SVR, sustained virological response. NS, not significant.
[a]*t* test.

previous cross-sectional studies revealed that the prevalence of group B infection is significantly higher in HCC cases than in non-HCC cases [Ogata et al., 2003], and that the group B infection is an independent risk factor for development of HCC in patients with chronic HCV infection [Nishise et al., 2007]. Second, NS3 interacts with host proteins associated with IFN signaling and thus influences cellular immunity. Since the serine protease encoded by the amino-terminal region of NS3 inhibits the IFN-signaling pathway, polymorphism of this region is likely to influence the effect of Peg-IFN/RBV combination therapy.

Several factors associated with the virological response to this therapy are well known, with adherence to both IFN and RBV strongly influencing outcome [Pearlman, 2004; Arase et al., 2005; Yamada et al., 2008]. In this study, we analyzed 75 cases in which >80% of the scheduled dosage of both drugs was administered. Of these cases, 28 (37%) and 40 (53%) were infected with group A and B isolates, respectively, which were similar rates to those for the 139 cases in the overall study. Age, gender, viral load before treatment, ALT level, proportion of fibrosis stage and adherence to Peg-IFN and RBV did not differ between the group A and B cases. However, the frequencies of SVR and EVR were significantly higher in group A, and those for non-EVR and non-SVR were significantly higher in group B. The results suggest that infection with the group B isolate, which correlates with a higher rate of HCC, is resistant to Peg-IFN/RBV therapy. The pre-treatment viremia status in the 68 cases with group A or B isolates showed no significant differences between the two groups of patients. Therefore, these results suggest that the secondary structure of the HCV NS3 amino-terminal region may be useful for prediction of the outcome of Peg-IFN/RBV combination therapy. In this initial study setting, the relationship of these polymorphisms to the frequency of rapid viral response at 4 weeks after the start of treatment was not evaluated. It will be important to assess this relationship in a future study.

The polymorphism in HCV core region (Arg70/Leu91) is a useful predictive marker for virological responses in Peg-IFN/RBV therapy [Akuta et al., 2007]. Interestingly, a combined analysis of polymorphisms of the core region (which encodes a structural protein) and HCV NS3 (a nonstructural protein) improved the prediction rate. Therefore, analysis of NS3 polymorphism in combination with the core structural polymorphism appears to improve prediction of the outcome of Peg-IFN/RBV therapy. A larger, multi-center prospective study would be necessary to validate the present results. In conclusion, the results of this study suggest that secondary structure polymorphism in the amino-terminal region of HCV NS3 is a useful predictive marker of the effect of Peg-IFN/RBV combination therapy for chronic hepatitis C. Although the present findings are clinically important, and will be helpful for predicting the outcome of Peg-IFN/RBV therapy, further in vitro studies will be needed to elucidate the molecular mechanism underlying the association of HCV NS3polymorphisms with clinical outcome.

REFERENCES

Akuta N, Suzuki F, Sezaki H, Suzuki Y, Hosaka T, Someya T, Kobayashi M, Saitoh S, Watahiki S, Sato J, Kobayashi M, Arase Y, Ikeda K, Kumada H. 2006. Predictive factors of virological non-response to interferon-ribavirin combination therapy for patients infected with hepatitis C virus of genotype 1b and high viral load. J Med Virol 78:83–90.

Akuta N, Suzuki F, Kawamura Y, Yatsuji H, Sezaki H, Suzuki Y, Hosaka T, Kobayashi M, Kobayashi M, Arase Y, Ikeda K, Kumada H. 2007. Predictive factors of early and sustained responses to peginterferon plus ribavirin combination therapy in Japanese patients infected with hepatitis C virus genotype 1b: Amino acid substitutions in the core region and low-density lipoprotein cholesterol levels. J Hepatol 46:403–410.

Arase Y, Ikeda K, Tsubota A, Suzuki F, Suzuki Y, Saitoh S, Kobayashi M, Akuta N, Someya T, Hosaka T, Sezaki H, Kobayashi M, Kumada H. 2005. Significance of serum ribavirin concentration in combination therapy of interferon and ribavirin for chronic hepatitis C. Intervirology 48:138–144.

Bruno S, Cammà C, Di Marco V, Rumi M, Vinci M, Camozzi M, Rebucci C, Di Bona D, Colombo M, Craxì A, Mondelli MU, Pinzello G. 2004. Peginterferon alfa-2b plus ribavirin for naïve patients with genotype 1 chronic hepatitis C: A randomized controlled trial. J Hepatol 41:474–481.

Deng L, Nagano-Fujii M, Tanaka M, Nomura-Takigawa Y, Ikeda M, Kato N, Sada K, Hotta H. 2006. NS3 protein of hepatitis C virus associated with the tumor suppressor p53 and inhibits its function in an NS3 sequence-dependent manner. J Gen Virol 87:1703–1713.

El-Shamy A, Sasayama M, Nagano-Fujii M, Sasase N, Imoto S, Kim SR, Hotta H. 2007. Prediction of efficient virological response to pegylated interferon/ribavirin combination therapy by NS5A sequences of hepatitis C virus and anti-NS5A antibodies in pre-treatment sera. Microbiol Immunol 51:471–482.

El-Shamy A, Nagano-Fujii M, Sasase N, Imoto S, Kim SR, Hotta H. 2008. Sequence variation in hepatitis C virus nonstructural protein 5A predicts clinical outcome of pegylated interferon/ribavirin combination therapy. Hepatology 48:38–47.

Enomoto N, Sakuma I, Asahina Y, Kurosaki M, Murakami T, Yamamoto C, Ogura Y, Izumi N, Marumo F, Sato C. 1996. Mutations in the nonstructural protein 5A gene and response to interferon in patients with chronic hepatitis C virus 1b infection. N Engl J Med 334:77–81.

Evans JD, Seeger C. 2006. Cardif: A protein central to innate immunity is inactivated by the HCV NS3 serine protease. Hepatology 43:615–617.

Foy E, Li K, Wang C, Sumpter R, Jr., Ikeda M, Lemon SM, Gale M, Jr. 2003. Regulation of interferon regulatory factor-3 by the hepatitis C virus serine protease. Science 300:1145–1148.

Gale MJ, Jr., Korth MJ, Tang NM, Tan SL, Hopkins DA, Dever TE, Polyak SJ, Gretch DR, Katze MG. 1997. Evidence that hepatitis C virus resistance to interferon is mediated through repression of the PKR protein kinase by the nonstructural 5A protein. Virology 230:217–227.

Gale MJ, Jr., Korth MJ, Katze MG. 1998. Repression of the PKR protein kinase by the hepatitis C virus NS5A protein: A potential mechanism of interferon resistance. Clin Diagn Virol 10:157–162.

Garnier J, Osguthorfe DJ, Robson B. 1978. Analysis of the accuracy and implications of simple methods for predicting the secondary structure of globular proteins. J Mol Biol 120:97–120.

Grandvaux N, Servant MJ, tenOever B, Sen GC, Balachandran S, Barber GN, Lin R, Hiscott J. 2002. Transcriptional profiling of interferon regulatory factor 3 target genes: Direct involvement in the regulation of interferon-stimulated genes. J Virol 76:5532–5539.

Hadziyannis SJ, Sette H, Jr., Morgan TR, Balan V, Diago M, Marcellin P, Ramadori G, Bodenheimer H, Jr., Bernstein D, Rizzetto M, Zeuzem S, Pockros PJ, Lin A, Ackrill AM. 2004. Peginterferon-alpha2a and ribavirin combination therapy in chronic hepatitis C: A randomized study of treatment duration and ribavirin dose. Ann Intern Med 140:346–355.

Hiramatsu N, Kurashige N, Oze T, Takehara T, Tamura S, Kasahara A, Oshita M, Katayama K, Yoshihara H, Imai Y, Kato M, Kawata S, Tsubouchi H, Kumada H, Okanoue T, Kakumu S, Hayashi N. 2008. Early decline of hemoglobin can predict progression of hemolytic anemia during pegylated interferon and ribavirin combination therapy in patients with chronic hepatitis C. Hepatol Res 38:52–59.

Ishido S, Hotta H. 1998. Complex formation of the nonstructural protein 3 of hepatitis C virus with the p53 tumor suppressor. FEBS Lett 438:258–262.

Kwun HJ, Jung EY, Ahn JY, Lee MN, Jang KL. 2001. p53-dependent transcriptional repression of p21(waf1) by hepatitis C virus NS3. J Gen Virol 82:2235–2241.

Manns MP, McHutchison JG, Gordon SC, Rustgi VK, Shiffman M, Reindollar R, Goodman ZD, Koury K, Ling M, Albrecht JK. 2001. Peginterferon alfa-2b plus ribavirin compared with interferon alfa-2b plus ribavirin for initial treatment of chronic hepatitis C: A randomized trial. Lancet 358:958–965.

Meylan E, Curran J, Hofmann K, Moradpour D, Binder M, Bartenschlager R, Tschopp J. 2005. Cardif is an adaptor protein in the RIG-I antiviral pathway and is targeted by hepatitis C virus. Nature 437:1167–1172.

Murphy MD, Rosen HR, Marousek GI, Chou S. 2002. Analysis of sequence configurations of the ISDR, PKR-binding domain, and V3 region as predictors of response to induction interferon-alpha and ribavirin therapy in chronic hepatitis C infection. Dig Dis Sci 47:1195–1205.

Nakaya T, Sato M, Hata N, Asagiri M, Suemori H, Noguchi S, Tanaka N, Taniguchi T. 2001. Gene induction pathways mediated by distinct IRFs during viral infection. Biochem Biophys Res Commun 283:1150–1156.

Nishise Y, Saito T, Sugahara K, Ito JI, Saito K, Togashi H, Nagano-Fujii M, Hotta H, Kawata S. 2007. Risk of hepatocellular carcinoma and secondary structure of hepatitis C virus (HCV) NS3 protein amino-terminus, in patients infected with HCV subtype 1b. J Infect Dis 196:1006–1009.

Nousbaum J, Polyak SJ, Ray SC, Sullivan DG, Larson AM, Carithers RL, Jr., Gretch DR. 2000. Prospective characterization of full-length hepatitis C virus NS5A quasispecies during induction and combination antiviral therapy. J Virol 74:9028–9038.

Ogata S, Ku Y, Yoon S, Makino S, Nagano-Fujii M, Hotta H. 2002a. Correlation between secondary structure of an amino-terminal portion of the nonstructural protein 3 (NS3) of hepatitis C virus and development of hepatocellular carcinoma. Microbiol Immunol 46:549–554.

Ogata S, Nagano-Fujii M, Ku Y, Yoon S, Hotta H. 2002b. Comparative sequence analysis of the core protein and its frameshift product, the F protein, of hepatitis C virus subtype 1b strains obtained from patients with and without hepatocellular carcinoma. J Clin Microbiol 40:3625–3630.

Ogata S, Florese RH, Nagano-Fujii M, Hidajat R, Deng L, Ku Y, Yoon S, Saito T, Kawata S, Hotta H. 2003. Identification of hepatitis C virus (HCV) subtype 1b strains that are highly, or only weakly, associated with hepatocellular carcinoma on the basis of the secondary structure of an amino-terminal portion of the HCV NS3 protein. J Clin Microbiol 41:2835–2841.

Pearlman BL. 2004. Hepatitis C treatment update. Am J Med 117:344–352.

Puig-Basagoiti F, Forns X, Furcić I, Ampurdanés S, Giménez-Barcons M, Franco S, Sánchez-Tapias JM, Saiz JC. 2005. Dynamics of hepatitis C virus NS5A quasispecies during interferon and ribavirin therapy in responder and non-responder patients with genotype 1b chronic hepatitis C. J Gen Virol 86:1067–1075.

Sakamuro D, Furukawa T, Takegami T. 1995. Hepatitis C virus nonstructural protein NS3 transforms NIH 3T3 cells. J Virol 69: 3893–3896.

Sarrazin C, Herrmann E, Bruch K, Zeuzem S. 2002. Hepatitis C virus nonstructural 5A protein and interferon resistance: A new model for testing the reliability of mutational analyses. J Virol 76:11079–11090.

Yamada K, Mori A, Seki M, Kimura J, Yuasa S, Matsuura Y, Miyamura T. 1998. Critical point mutations for hepatitis C virus NS3 proteinase. Virology 246:104–112.

Yamada G, Iino S, Okuno T, Omata M, Kiyosawa K, Kumada H, Hayashi N, Sakai T. 2008. Virological response in patients with hepatitis C virus genotype 1b and a high viral load: Impact of peginterferon-alpha-2a plus ribavirin dose reductions and host-related factors. Clin Drug Investig 28:9–16.